degree of ionization, the half-life of the LSI decrease became longer. This is shown in Figure 7.

In conclusion, the results obtained in this work appear to indicate that chain expansion of PMA in methanol induced by a sudden increase in the degree of ionization does not occur as a cooperative process but instead as a stepwise process involving initially only the outer regions of the coils. This takes place in the microsecond time range. Subsequently, a statistical distribution of ionized sites is established in a rather slow equilibration process. The relaxation process observed by Morawetz et al.[3] in the time range of seconds probably corresponds to this equilibration process. Attempts to detect the slow process in the present work were not successful because the light scattering setup did not allow measurements of small LSI changes at long time scales.

Acknowledgment. The poly(methacrylic acid) samples were synthesized and characterized by R. Zuch, U. Fehrmann, and M. Weller at the Hahn-Meitner-Institut. The valuable assistance of Dr. G. Beck during the flash photolysis experiments is gratefully acknowledged.

References and Notes

(1) Irie, M.; Schnabel, W. *Makromol. Chem., Rapid Commun.* **1984**, *5*, 413.
(2) Irie, M. *J. Am. Chem. Soc.* **1983**, *105*, 2078.
(3) Bednar, B.; Morawetz, H.; Shafer, J. A. *Macromolecules* **1985**, *18*, 1940.
(4) Schnabel, W. In *Developments in Polymer Degradation*; Grassie, N., Ed.; Elsevier Applied Science: London, 1979; Vol. 2.
(5) Beck, G. *Rev. Sci. Instrum.* **1979**, *50*, 1147.
(6) Tanford, C. *Physical Chemistry of Macromolecules*; Wiley: New York, 1957; p 482.
(7) Oosawa, F. *Polyelectrolytes*; Marcel Dekker: New York, 1971.
(8) Morawetz, H. *Macromolecules in Solution*, 2nd ed.; Wiley: New York, 1975; p 344.
(9) Trementozzi, Q. A. *J. Am. Chem. Soc.* **1954**, *76*, 5293.
(10) Rouse, P. E. *J. Chem. Phys.* **1953**, *21*, 1272.
(11) Zimm, B. H. *J. Chem. Phys.* **1956**, *24*, 269.
(12) Wiederhorn, N. M.; Brown, A. R. *J. Polym. Sci.* **1952**, *8*, 651.
(13) Adachi, K.; Kotaka, T. *Macromolecules* **1983**, *16*, 1936.

Fiber Spinning from the Nematic Melt. 3. The Copolyester of *p*-Hydroxybenzoic Acid and 2-Hydroxy-6-naphthoic Acid

Hiromochi Muramatsu† and W. R. Krigbaum*

Department of Chemistry, Duke University, Durham, North Carolina 27706.
Received May 27, 1986

ABSTRACT: Rheological measurements and fiber spinning were performed for the copolyester of *p*-hydroxybenzoic acid and 2-hydroxy-6-naphthoic acid furnished by Celanese Corp. This polymer softens at 222 °C and the DSC melting endotherm occurs at 247 °C. Fibers were spun from the melt at temperatures of 250, 260, and 280 °C, taking the spin draw ratio as a variable at each temperature. The initial modulus, breaking tenacity, and elongation to break were measured. The structure of the fibers was characterized by wide-angle X-ray diffraction and differential scanning calorimetry measurements. The initial modulus, M_0, for fibers spun at 260 or 280 °C increases strongly at low spin draw ratios and reaches a plateau value, about 425 g/denier, at a spin draw ratio of 135. This is over twice the value we obtained for the copolyester of poly(ethylene terephthalate) containing 60 mol % *p*-oxybenzoate units. The initial modulus of fibers spun at 250 °C increases more slowly with spin draw ratio and reaches a plateau value of only 220 g/denier at a spin draw ratio of 60. The breaking tenacity of fibers spun at 260 or 280 °C exhibits a sharp peak when plotted as a function of the spin draw ratio. When the melt was preheated to 280 °C before spinning at 250 °C, the fiber properties coincided with those of fibers spun at 260 or 280 °C without preheating. Heat treatment of the fibers increases the inherent viscosity, the degree of crystallinity, and the crystal melting temperature. However, heat treatment improves the fiber properties only if the spin draw ratio is high, but not for fibers collected at low spin draw ratios. These findings are discussed in terms of the crystallite orientation, degree of crystallinity, and rheological properties.

Introduction

Thermotropic liquid crystal polyesters have attracted considerable attention due to their ease of processing and good mechanical properties. One of the earliest of these to become available in quantity is the copolymer of poly(ethylene terephthalate) and *p*-hydroxybenzoic acid supplied by Tennessee Eastman Co.[1-3] The rheological[1-11] and fiber properties[1,2,11-15] of this polymer have been investigated by a number of workers. More recently, a series of thermotropic polyesters disclosed by Calundann[16,17] has become commercially available from Celanese Corp. One of these is a random copolymer of *p*-hydroxybenzoic acid and 2-hydroxy-6-naphthoic acid, which we will designate as HBA/HNA. Blackwell and co-workers[18-20] studied the molecular structure of this polymer by X-ray diffraction. They reported good agreement between the observed *d* spacings of the meridional reflections and those calculated under the assumption that the sequence of monomers is random. Stamatoff[21] and Donald and Windle and co-workers[22-24] studied the effect of annealing upon the texture. There appears to be some rearrangement in packing but no development of three-dimensional order in this copolymer. Blundell[25] has estimated a crystallinity of about 20% for the copolymer containing 60 mol % HNA. On the other hand, Butzbach and co-workers,[26] from thermal studies, predicted a long-range three-dimensional order and a high degree of crystallinity. Only a few studies of the behavior in fiber spinning have been reported.[16,17,27,28]

Experimental Section

The random copolyester of *p*-hydroxybenzoic acid (HBA) and 2-hydroxy-6-naphthoic acid (HNA) containing 42 mol % HNA was kindly supplied by Celanese Corp. We will designate this

† Permanent address: Nippondenso Co., Ltd., Research and Development Department 1, 1-1 Showa-cho, Kariya-city, Aichi Prefecture, Japan.

0024-9297/86/2219-2850$01.50/0

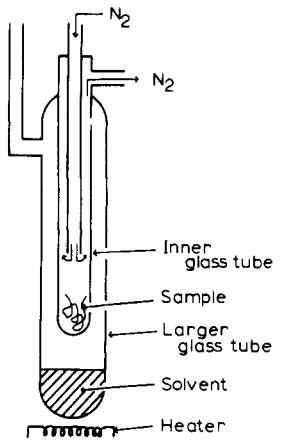

Figure 1. Schematic diagram of the apparatus for heat treating fibers.

copolymer as HBA/42HNA. The polymer chips were dried overnight at 110 °C in a vacuum oven before use. Inherent viscosities were determined at 50 °C in 0.07 wt % tetrafluorophenol solutions using a Ubbelohde viscometer. Thermal transitions were studied with a DuPont 1090 DSC using 4–6-mg sample size and a heating rate of 10 °C min. An Olympus BH-2 polarizing microscope equipped with a Mettler FP5 hot stage was used to follow texture changes.

Rheometry. Rheological measurements were performed with a Sieglaff–McKelvey capillary rheometer using a capillary 25 mm in length and having a length to diameter ratio, L/D, of 88.9. No corrections were applied to the apparent shear rate. Experiments were performed at 240, 250, 260, and 280 °C, using a new sample and cleaned barrel for each temperature. To study the effect of thermal history, the polymer was heated to 260 °C for 20 min and cooled to the measurement temperature, either 240 or 250 °C, during 22 min. The sample was maintained at the measurement temperature for an additional 5–25 min to ensure that thermal equilibrium was achieved. To avoid the introduction of moisture, a continuous stream of nitrogen was introduced over the upper part of the barrel during the measurements, as suggested by Wissbrun and Zahorchak.[29]

Spinning. Melt spinning was performed with the Sieglaff–McKelvey rheometer using a capillary 25 mm in length and having an L/D ratio of 49.4. The spinning temperatures were 250, 260, and 280 °C. The shear rate at the wall, after application of Bagley[30] and Weissenberg–Rabinowitsch[31] corrections, was 115 s^{-1}. The spun fiber was collected with a take-up machine located 1.0 m below the capillary. The spin draw ratio, V_f/V_0, was determined by measuring the decrease in diameter of the fiber. The fiber was photographed and its diameter determined microscopically by comparison with a photograph of a calibrated reticle taken at the same magnification. Die swell was assumed to be negligible, so the diameter of the fiber with spin draw ratio 1.0 was taken as the diameter of the spinneret furnished by the manufacturer. Fibers with approximately unit spin draw ratio were obtained as described in an earlier paper.[14]

The stress–strain curve was determined by using an Instron Model 1130 with a sample length of 2 in. and a strain rate of 5 in./min. Values of the initial modulus, breaking tenacity, and elongation to break are the averages taken from six stress–strain curves. Wide-angle X-ray diffraction patterns were collected with a flat-plate camera and nickel-filtered Cu Kα radiation. The sample-to-film distance was calibrated with silicon powder.

Fibers were heat treated in an inert-gas environment using the apparatus illustrated in Figure 1. The fiber was placed in the inner glass tube, which was connected to a nitrogen tank. This tube was inserted in the larger tube containing *n*-decyl alcohol, which boils at 231 °C. This temperature is approximately 15 °C below the melting point of the polymer. Nitrogen gas was introduced into the inner tube for 60 min before heating was begun. The liquid was heated to its boiling temperature and the vapor heated the inner tube. The flow of nitrogen gas in the inner tube was continued during heating and as the fiber was cooled to room temperature.

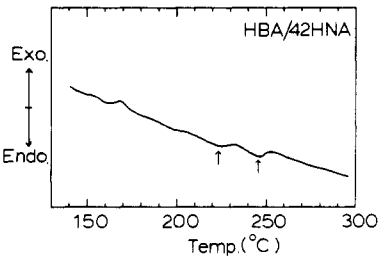

Figure 2. DSC heating curve of HBA/42HNA recorded at 10°/min.

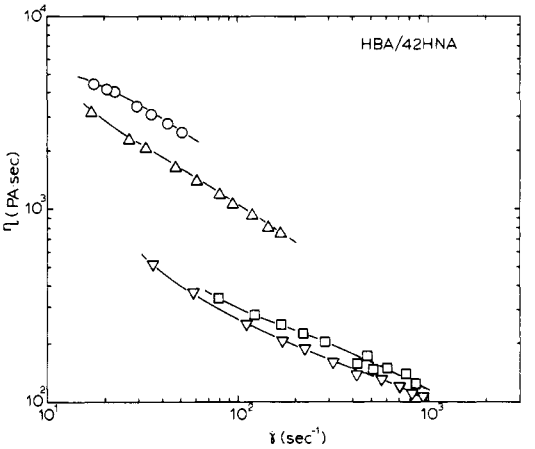

Figure 3. log–log plot of the melt viscosity as a function of apparent shear rate. Temperatures are 240 (○), 250 (△), 260 (□), and 280 °C (▽).

Results

The differential scanning thermogram of HBA/42HNA shown in Figure 2 indicates two endotherms above 200 °C. These are located at 222 and 247 °C. The latter agrees reasonably well with the melting temperature of 245 °C reported by Calundann[16] for HBA/40HNA. The slight difference may arise from the difference in composition. Examination with the polarizing microscope indicated that the polymer softens at 222 °C and becomes fluid at 247 °C. The molten polymer appeared bright under crossed polars and was easily oriented along the flow direction when pressure was applied to the cover slip.

In Figure 3 the melt viscosity measured at four temperatures is plotted as a function of the apparent shear rate using a log–log plot. The viscosity decreases with temperature at a given shear rate, and the most rapid decrease occurs between 250 and 260 °C, which suggests some crystallites are present that melt above the 247 °C temperature of the DSC melting endotherm. The effect of thermal history upon melt viscosity is illustrated in Figure 4. The open triangles represent the flow curve measured at 250 °C without preheating, while the filled triangles represent the viscosity of a melt that had been heated to 260 °C for 20 min, cooled to 250 °C during 22 min, and maintained at that temperature 15 min to ensure thermal equilibrium. It required 20–30 min for the viscosity measurements. The viscosity of the preheated sample is reduced by a factor of 0.3 and very nearly corresponds to the viscosity curve for 260 °C (open squares). A reduction of melt viscosity due to preheating was reported by Wissbrun,[4] Cogswell,[32] Wissbrun and Ide,[33] and Muramatsu and Krigbaum.[15] A second preheating experiment was run for a measuring temperature of 240 °C. The open circles indicate the flow curve measured at 240 °C without preheating, while the filled circles represent viscosities measured after the sample was heated to 260

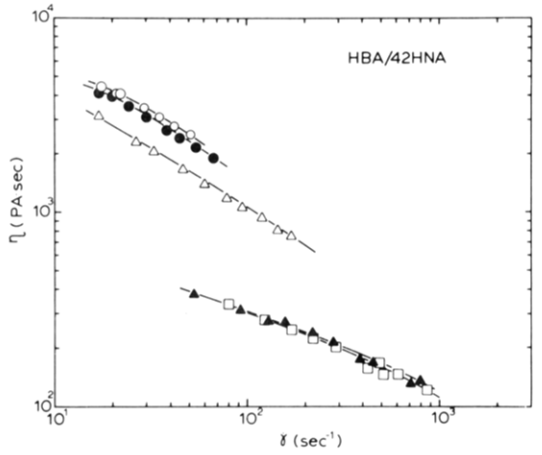

Figure 4. Effect of preheating on the melt viscosity. Melt viscosity vs. shear rate for temperatures 240 °C (○), 260 °C (□), 240 °C after preheating the melt to 260 °C (●), 250 °C (△), and 250 °C after preheating the melt to 260 °C (▲).

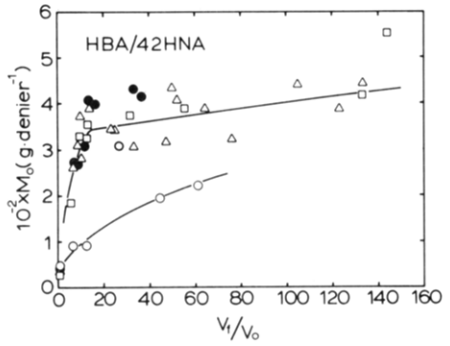

Figure 5. Initial modulus plotted as a function of spin draw ratio for fibers spun at 250 °C (○), 260 °C (△), 280 °C (□), and 250 °C after preheating the melt to 280 °C (●).

°C for 20 min, cooled to 240 °C during 22 min, and maintained at this temperature for an additional 25 min to obtain thermal equilibrium. The reduction of viscosity is quite small, indicating that crystallization occurs in the melt on the time scale of these measurements between 240 and 250 °C.

Fibers were spun at a wall shear rate of 115 s^{-1} using a capillary 25 mm in length and having an L/D ratio of 49.4. The spinning temperatures were 250, 260, and 280 °C. In Figure 5 the initial modulus, M_0, is shown plotted as a function of the spin draw ratio, V_f/V_0, for fibers spun at these three temperatures. Although there is considerable scatter, the data are adequately represented by two curves. The initial modulus of fibers spun at 250 °C (open circles) is low and increases gradually with spin draw ratio. For spinning temperatures of 260 and 280 °C the initial moduli are higher and increase more rapidly with spin draw ratio up to V_f/V_0 about 15. Above this spin draw ratio the increase is more gradual. Alderman and Mackley[28] reported that the initial modulus of fibers spun at 295 °C reached a plateau value at a spin draw ratio of slightly over 2. The filled circles in Figure 5 represent initial modulus of fibers spun at 250 °C after the melt had been heated to 280 °C. These values fall on the curve of fibers spun at 260 or 280 °C without preheating, indicating that better orientation was obtained by preheating the melt, which melted preexisting crystallites. These results resemble those obtained in our earlier study[15] of the copolyester of poly(ethylene terephthalate) containing 60 mol % *p*-oxybenzoate units.

Figure 6 illustrates the dependence of initial modulus on fiber denier for fibers spun at three temperatures

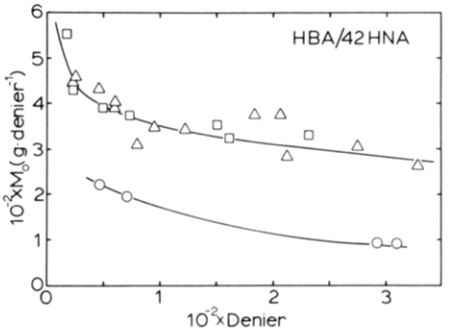

Figure 6. Initial modulus vs. denier per filament for fibers spun at 250 (○), 260 (△), and 280 °C (□).

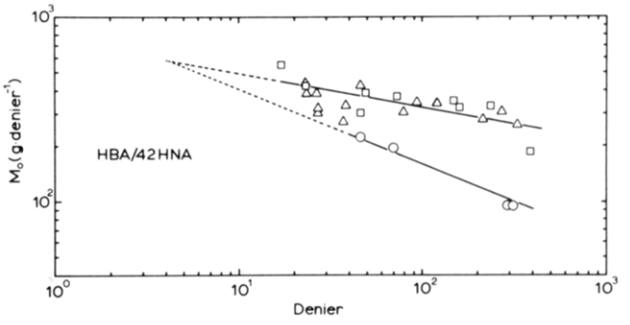

Figure 7. log–log plot of initial modulus vs. denier per filament for three spinning temperatures. Symbols have same significance as in Figure 6.

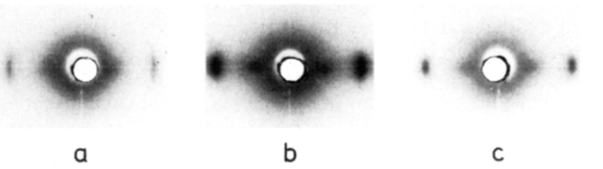

Figure 8. X-ray diffraction patterns (a) of fibers spun at 250 °C with spin draw ratio 61, (b) of fibers spun at 260 °C with spin draw ratio 52, and (c) of fibers spun at 280 °C with spin draw ratio 56.

without preheating the melt. Again, the data are adequately represented by two curves. The lower curve represents the initial modulus of fibers spun at 250 °C, while the upper curve indicates the modulus of fibers spun at 260 or 280 °C. This result indicates that the differences seen in Figure 5 cannot be ascribed to differences in denier. We conclude that orientation is improved when the spinning temperature is high enough to melt all crystallites. Figure 7 shows a log–log plot of initial modulus vs. denier, which appears to be a linear relationship. Calundann[16] reported an initial modulus of 597 g/denier for a 4-denier fiber. We were unable to achieve the spin draw ratio necessary to obtain such a small denier with our single filament spinneret. However, extrapolation of the linear relations in Figure 7 gives an initial modulus of about 590 g/denier for a 4-denier fiber. This is in agreement with Calundann's value. Rather surprisingly, this same value is predicted for a fiber spun at 250 °C. This does not indicate, of course, that the spin draw ratio required to produce that denier could be achieved for fibers spun at 250 °C.

The data in Figures 5 and 6 demonstrate that orientation in the fiber is more complete when the melt contains no crystallinity. This conclusion is confirmed by the X-ray diagrams of as-spun fibers shown in Figure 8. The WAXS patterns of fibers spun at 250 °C indicate poor orientation at all spin draw ratios relative to that achieved by spinning at 260 or 280 °C.

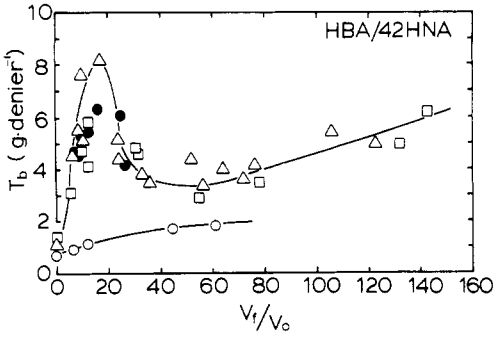

Figure 9. Breaking tenacity vs. spin draw ratio for fibers spun at 250 °C (○), 260 °C (△), 280 °C (□), and 250 °C following preheating to 280 °C (●).

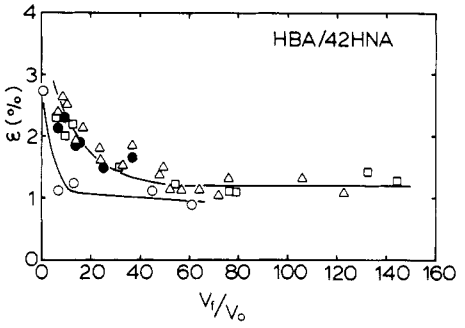

Figure 10. Elongation to break vs. spin draw ratio for fibers spun at three temperatures without preheating. Symbols are the same as in Figure 9.

The breaking tenacity, T_b, is shown as a function of spin draw ratio in Figure 9. Values obtained for fibers with spin draw ratio unity are shown near the ordinate. The breaking tenacity is quite low for fibers spun at 250 °C and only increases slowly with spin draw ratio. Fibers spun at 260 or 280 °C exhibit quite a different behavior. The breaking tenacity increases to a maximum at a spin draw ratio of approximately 15, decreases to a minimum at a spin draw ratio of 45, and finally increases more slowly with further increase in spin draw ratio. The spin draw ratio of 15, corresponding to that giving the highest breaking tenacity, coincides with the spin draw ratio at which the initial modulus changes slope, as shown in Figure 5. We also note that when the melt is preheated to 280 °C before spinning at 250 °C, the behavior of the breaking tenacity corresponds to that of fibers spun at the higher temperature rather than to fibers spun at 250 °C without preheating. Our observations for the breaking tenacity differ from those of Calundann and Jaffe,[27] who reported a monotonic increase of tenacity with spin draw ratio. As shown in Figure 10, elongation to break, ϵ, decreases with increasing spin draw ratio. Fibers spun without preheating at 250 °C exhibit lower elongation to break. Fibers spun at 260 or 280 °C without preheating have larger elongation to break values, and the plateau value appears to be reached at a spin draw ratio of approximately 45. Again, fibers spun at 250 °C after preheating to 280 °C exhibit properties in agreement with those of fibers spun at the two higher temperatures.

Heat Treatment of Fibers. Luise[34] disclosed that the mechanical properties of well-oriented fibers could be improved by heat treatment. This improvement was ascribed to an increase in polymer molecular weight and improvement in the crystallite orientation. Figure 11 illustrates values of the initial modulus of fibers that had been heat treated at 231 °C plotted against the time of heat treatment on a logarithmic scale. Improvement in the initial

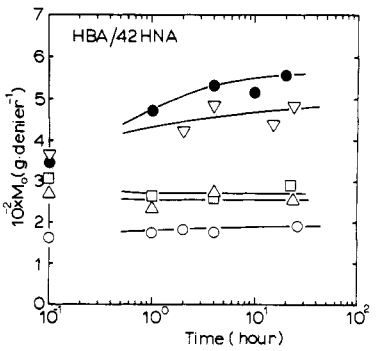

Figure 11. Initial modulus plotted as a function of fiber heat treatment time for fibers spun at 260 °C and spin draw ratios 5.8 (○), 12.2 (△), 36 (□), 44 (▽), and 68 (●).

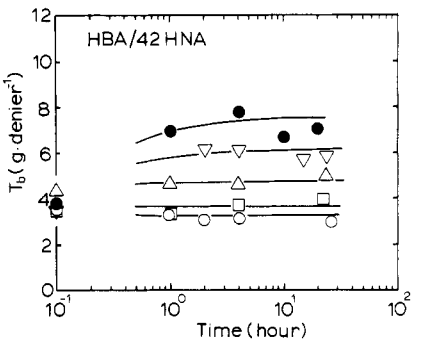

Figure 12. Breaking tenacity vs. fiber heat treatment time for fiber spun at 260 °C. Symbols are the same as in Figure 11.

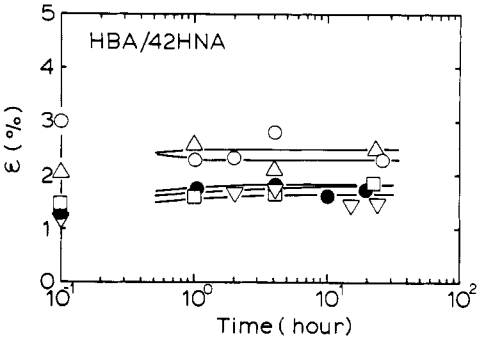

Figure 13. Elongation to break vs. heat treatment time for fibers spun at 260 °C. Symbols are the same as in Figure 11.

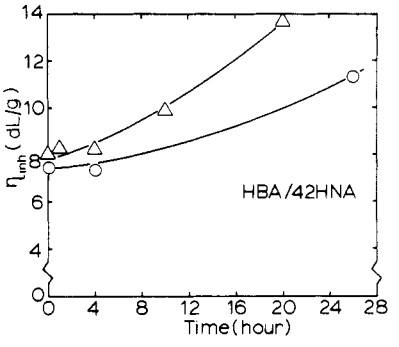

Figure 14. Inherent viscosity vs. heat treatment time for fibers spun at 260 °C and at spin draw ratios 5.8 (○) and 68 (△).

modulus appears to be a function of the orientation initially present in the fiber. The largest increase is shown by fibers with a spin draw ratio of 68, while there appears to be no improvement for fibers with spin draw ratios of 36 or less. The breaking tenacity is shown in Figure 12 plotted against the logarithm of the heat treatment time. Again, this property is improved for fibers collected with

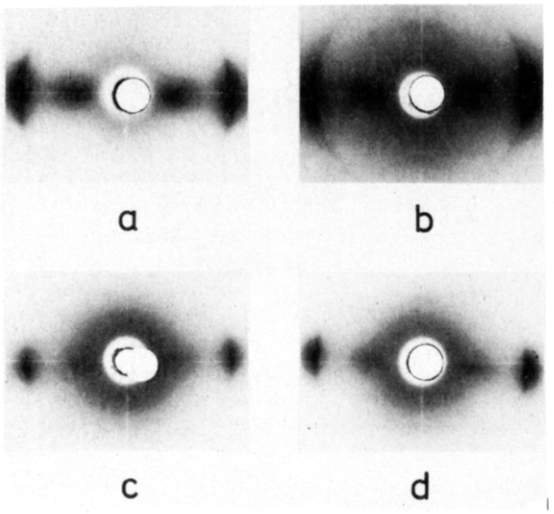

Figure 15. X-ray diffraction patterns of fibers spun at 260 °C. Spin draw ratio 5.8 and heat treatment time (a) 0 and (b) 20 h. Spin draw ratio 68 and heat treatment time (c) 0 and (d) 20 h.

larger spin draw ratios, but no improvement is evident for those fibers with spin draw ratios of 36 or less. Elongation to break for the heat treated fibers is illustrated in Figure 13. There is only a modest improvement for spin draw ratios of 68 and 49, but no increase for fibers with lower spin draw ratios. Figure 14 shows the inherent viscosity values of fibers with spin draw ratios of 5.8 (circles) and 68 (triangles) as a function of heat treatment time. The inherent viscosity of the fiber with spin draw ratio 5.8 increased from 7.5 to 11.3 dL/g after 26 h of heat treatment. This value is larger than that of the fiber with spin draw ratio 68 after 10 h of heat treatment. Despite this increase in inherent viscosity, the fiber with spin draw ratio 5.8 did not exhibit any improvement in mechanical properties while, as shown in Figures 11 and 12, the initial modulus and breaking tenacity of the fiber with spin draw ratio 68 improved significantly after 10 h of heat treatment. It should be noted that the heat treatment described by Luise[34] involves heating the fiber for a period of time at successively higher temperatures. We have used only the first step of this process. Had we heated for an hour at higher temperatures, the changes in mechanical properties would have been larger, but we believe the conclusions reached in our study of heat treatment would not have been altered.

Figure 15 illustrates the WAXS patterns of fibers after heat treatment. For all spin draw ratios, the degree of crystallinity was increased by heat treatment. To obtain a more quantitative estimate of the change in crystallinity due to heat treatment, DSC curves were collected for treated fibers. The upper set of curves in Figure 16 shows the DSC heating curves of fibers having spin draw ratio 5.8 before and after heat treatment. The temperature of the major melting endotherm is increased from about 250 °C (no heat treatment) to 268 °C after heat treatment for 26 h. Also, the area of the melting endotherm increased significantly, indicating an increase in the degree of crystallinity. The lower set of three heating curves represents fibers with spin draw ratio 68. In this case heat treatment increases the temperature of the major melting endotherm from 243 to 268 °C, and the area of the melting endotherm is enlarged. Figure 17 illustrates the variation of the endotherm melting temperature as a function of heating time for both fibers. The increase is somewhat more rapid for the fiber with the larger spin draw ratio, but clearly the perfection of the crystals is improved by heat treatment of both fibers. We conclude from these

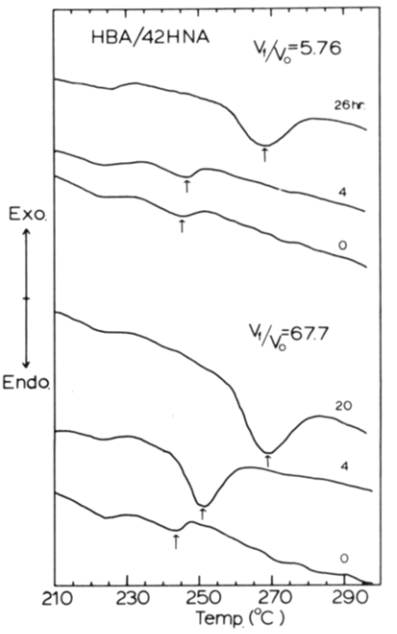

Figure 16. DSC heating curves taken at a scanning rate of 10 °C/min for fibers spun at 260 °C and spin draw ratio 5.8 with three fiber heat treatment times (upper three curves) and for spin draw ratio 68 at three indicated fiber heat treatment times (three lower curves).

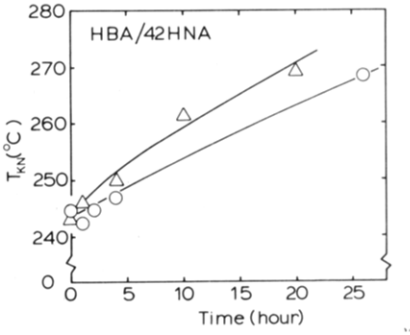

Figure 17. Crystal melting temperature (DSC endotherm) vs. fiber heat treatment time for fibers spun at 260 °C and with spin draw ratio 5.8 (○) and 68 (△).

results that the improvement in mechanical properties upon heat treatment cannot be explained solely by an increase of polymer molecular weight, by an increase in the degree of crystallinity, or by an improvement in crystal perfection leading to higher melting temperatures.

Discussion

Acierno and co-workers[12] investigated the mechanical properties of fibers spun from PET/60PHB. They reported a discontinuity in the plots of T_b and ϵ vs. spin draw ratio. They offered the explanation that these discontinuities were due to orientation of the amorphous regions of the polymer. In this study of HBA/42HNA no discontinuity was observed, although the tenacity exhibited a maximum as a function of spin draw ratio. These results can be explained as follows. At very low spin draw ratios the fiber has low orientation and low modulus, as shown in Figure 5. There are many entanglements. The initial modulus increases with increasing spin draw ratio due to the development of better orientation. The improvement in initial modulus becomes slower at a spin draw ratio of 15, and the breaking tenacity reaches a maximum at the same spin draw ratio, as can be seen in Figure 9. These changes are due to the fact the chains are now nearly fully extended and parallel, and the number of entanglements is reduced. With further increase in spin draw ratio, the

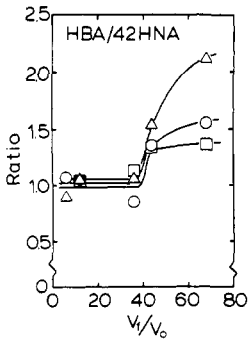

Figure 18. Ratio of the breaking tenacity (△), initial modulus (○), and elongation to break (□) for fibers heat treated 4 h at 231 °C to that for a fiber without heat treatment plotted against spin draw ratio of the fiber.

orientation becomes somewhat better and the lateral packing of the chains improves. For spin draw ratios above 45 the initial modulus and elongation to break approximate their plateau values, but the breaking tenacity again increases due to the improvement in lateral packing of the chains.

When the fiber was spun from a melt that had been preheated to 280 °C before cooling to the spinning temperature of 250 °C, the mechanical properties were improved. As shown in Figure 4, preheating reduces the viscosity of the melt at 250 °C. The initial modulus for the fiber spun at 250 °C after preheating at 280 °C is increased, as indicated by the filled circles in Figure 5, and approximates the values obtained by spinning at the preheating temperature. The breaking tenacity also increased, as shown by the filled circles in Figure 9, and exhibits a peak when plotted against spin draw ratio. These features are also exhibited by fibers spun at 260 or 280 °C without preheating the melt. Some crystallinity must be present at temperatures below 260 °C, as indicated by the drop in melt viscosity between 250 and 260 °C in Figure 3. Preheating at or above 260 °C removes these crystals and reduces the melt viscosity, which improves the molecular orientation in the fiber.

Heat treatment of the fiber increases the degree and perfection of crystallites (and thus the polymer melting temperature) and also increases the molecular weight of the polymer. Figure 18 shows the ratio of the mechanical properties of a fiber heat treated 4 h at 231 °C to those of a fiber having no heat treatment. This clearly demonstrates that the fiber properties are only improved by heat treatment if the spin draw ratio exceeds 45. Hence the fiber must be highly oriented prior to heat treatment if that treatment is to improve the mechanical properties of the fiber. The tenacity reached a minimum at a spin draw ratio of 45, and the elongation to break reached its plateau value. These observations suggest that the fiber is approaching its optimum orientation at this spin draw ratio.

Acknowledgment. We are pleased to acknowledge support of this work by the Army Research Office (Grant DAA29-84-0033). We also wish to express our appreciation to Celanese Corp. for supplying the sample of the polymer used in this work and to Dr. C. K. Liu of this laboratory for helpful discussions.

Registry No. (HBA)(HNA) (copolymer), 81843-52-9.

References and Notes

(1) Kuhfuss, F.; Jackson, W. J., Jr. U.S. Patent 3 778 410, 1973.
(2) Kuhfuss, F.; Jackson, W. J., Jr. U.S. Patent 3 804 805, 1974.
(3) Jackson, W. J., Jr.; Kuhfuss, F. *J. Polym. Sci., Polym. Chem. Ed.* **1976**, *14*, 2043.
(4) Wissbrun, K. F. *Br. Polym. J.* **1980**, *12*, 163.
(5) White, J. L.; Fellers, J. F. *J. Appl. Polym. Sci. Appl. Polym. Symp.* **1978**, *33*, 137.
(6) Jerman, R. E.; Baird, D. G. *J. Rheol.* **1981**, *25*, 275.
(7) Wissbrun, K. F. *J. Rheol.* **1981**, *25*, 619.
(8) Wissbrun, K. F. Paper presented at the AIChE Meeting, Houston, TX, Mar 27–30, 1983.
(9) Baird, D. G. In *Polymer Liquid Crystals*; Blumstein, A., Ed.; Plenum: New York, 1983; pp 119–143.
(10) Gotsis, A. D.; Baird, D. G. *J. Rheol.* **1985**, *29*, 539.
(11) Sugiyama, H.; Lewis, D. N.; White, J. L.; Fellers, J. F. *J. Appl. Polym. Sci.* **1985**, *30*, 2329.
(12) Acierno, D.; La Mantia, F. P.; Polizzotti, G.; Ciferri, A.; Valenti, B. *Macromolecules* **1982**, *15*, 1455.
(13) Chen, G. M.S. Thesis, Department of Textile Chemistry, North Carolina State University, Raleigh, NC, 1985.
(14) Muramatsu, H.; Krigbaum, W. R. *J. Polym. Sci., Polym. Phys. Ed.* **1986**, *24*, 1695.
(15) Muramatsu, H.; Krigbaum, W. R. *J. Polym. Sci., Polym. Phys. Ed.*, in press.
(16) Calundann, G. W. U.S. Patent 4 161 470, 1979.
(17) Calundann, G. W. U.S. Patent 4 184 996, 1980.
(18) Gutierrez, G. A.; Chivers, R. A.; Blackwell, J.; Stamatoff, J. B.; Yoon, H. *Polymer* **1983**, *24*, 937.
(19) Gutierrez, G. A.; Blackwell, J.; Chivers, R. *Polymer* **1985**, *26*, 348.
(20) Chivers, R. A.; Blackwell, J. *Polymer* **1985**, *26*, 997.
(21) Stamatoff, J. B. *Mol. Cryst. Liq. Cryst.* **1980**, *110*, 75.
(22) Donald, A. M.; Windle, A. H. *Polymer* **1984**, *25*, 1235.
(23) Donald, A. M.; Windle, A. H. *J. Mater. Sci., Lett.* **1985**, *4*, 58.
(24) Windle, A. H.; Viney, C.; Golombok, R.; Donald, A. M.; Mitchell, G. R. *Faraday Discuss. Chem. Soc.* **1985**, *79*, 55.
(25) Blundell, D. L. *Polymer* **1982**, *23*, 359.
(26) Butzbach, G. D.; Wendorff, J. H.; Zimmerman, N. J. *Macromol. Chem., Rapid Commun.* **1985**, *6*, 821.
(27) Calundann, G. W.; Jaffe, M. *Proc. Robert A. Welch Found., Conf. Chem. Res.* **1982**, *26*, 247.
(28) Alderman, J.; Mackley, M. R. *Faraday Discuss. Chem. Soc.* **1985**, *79*, 149.
(29) Wissbrun, K. F.; Zahorchak, A. C. *J. Polym. Sci., Part A-1* **1971**, *9*, 2093.
(30) Bagley, E. B. *J. Appl. Phys.* **1957**, *28*, 624; *Trans. Soc. Rheol.* **1961**, *5*, 355.
(31) Rabinowitsch, B. *J. Phys. Chem.* **1929**, *A145*, 1.
(32) Cogswell, F. N. *Br. Polym. J.* **1980**, *12*, 170.
(33) Wissbrun, K. F.; Ide, Y. U.S. Patent 4 325 903, 1982.
(34) Luise, R. R. U.S. Patent 4 247 514, 1981.